Indian Journal of Chemistry
Vol. 64, August 2025, pp. 836-845
DOI: 10.56042/ijc.v64i8.18610

Synthesis, anticancer evaluation, and molecular docking studies of vanillin-2,4-thiazolidinedione-triazole hybrid analogues

B Ravali[b#], A Niranjana Kumar[a#], Pooja Jagdale[f], Akanksha Singh[c,e], Ankush Bansode[f], J Kotesh Kumar*[a], K V N Satya Srinivas*[a], Santosh Kumar Guru[f], B Balakishan[d], Abha Meena[c] & B Venkatesh[a]

[a] Phytochemistry Division, CSIR-Central Institute of Medicinal and Aromatic Plants, Research Centre, Boduppal, Hyderabad 500 092, India

[b] Department of Pharmaceutical Chemistry, G. Pulla Reddy College of Pharmacy, Hyderabad 500 028, India

[c] Bioprospection and Product Development Division, CSIR-Central Institute of Medicinal and Aromatic Plants, Lucknow 226 015, Uttar Pradesh, India

[d] NMR Division, CSIR-Central Institute of Medicinal and Aromatic Plants, Lucknow 226 015, Uttar Pradesh, India

[e] Academy of Scientific and Innovative Research (AcSIR), CSIR-HRDC Campus, Postal Staff College Area, Sector 19, Kamla Nehru Nagar, Ghaziabad 201 002, Uttar Pradesh, India

[f] Department of Biological Sciences (Pharmacology and Toxicology), National Institute of Pharmaceutical Education and Research (NIPER), Hyderabad, Telangana 500 037, India

E-mail: koteshkumarj@cimap.res.in, kvn.satyasrinivas@cimap.res.in

Received 7 April 2025; accepted (revised) 29 July 2025

Ten novel vanillin-2,4-thiazolidinedione-triazole hybrid analogues have been synthesized *via* Knoevenagel condensation and 1,3-dipolar cycloaddition. These have been tested for *in vitro* anticancer activity against various human cancer cell lines, including MDA-MB 231, MCF-7, A549, and FaDU. Compound **7f** (flouro and bromo substituted) shows notable inhibition of MDA-MB 231 (50.61%; IC30: 21.98 µm), while compound **7i** (di-flouro substituted) significantly inhibits FaDU (52.08%; IC30: 23.57 µm). *In silico* studies demonstrate that **7f** and **7i** have strong binding affinity with SDH (–16.7, –16.5), BCL-2 (–13.7, –13.7), BCL-XL (–16.2, –16.9) and BCL-W (–17.8, –17.7). These results suggest that such hybrid heterocyclic systems might be promising candidates for new anticancer therapies.

Keywords: Vanillin, 2,4-Thiazolidinedione, 1,2,3-Triazole, Anticancer activity, Molecular docking, Toxicity

Vanillin (**1**), a phenolic aldehyde, is the primary component responsible for the characteristic flavor and aroma of vanilla (*Vanilla planifolia*). Vanillin is found in cured vanilla beans at a concentration of 1.0–2.0% w/w[1]. It is derived from three primary sources: natural[2], chemical/synthetic[3,4], and biotechnological processes. Depending on its origin and production method, vanillin is categorized as either a natural or artificial flavor. Beyond its well-known flavor and aroma, vanillin exhibits a broad spectrum of bioactive properties. Emerging studies highlight its potential as a medicinal molecule, further enhancing its appeal for healthcare applications. Moreover, its inclusion on the Generally Recognized as Safe (GRAS) list of food additives underscores its safety and versatility.

In addition to its characteristic flavor and aroma, vanillin possesses a range of bioactive properties, including anticancer[5], neuroprotective[6], sickle cell anemia treatment[7], antioxidant and anti-inflammatory[8,9], antifungal[10], antibacterial[11], cosmeceutical applications[12], and wound healing potential[13].

Furthermore, various classes of vanillin derivatives have been reported in the literature, exhibiting enhanced pharmacological activities compared to the parent molecule. These derivatives demonstrate diverse biological effects, including amino-vanillins with antioxidant properties[14], acetyl vanillins with antimicrobial potential[15], tacrine- or naphthalimido-vanillins as acetylcholinesterase enzyme inhibitors[16], bis(2-hydroxyethyl)-dithioacetal-vanillins effective against potato and cucumber mosaic viruses[17], and 1,3,4-thiadiazole vanillins with antibacterial activity[18], among others.

2,4-Thiazolidinediones (TZDs) are composed of a five-membered ring containing sulphur and nitrogen as heteroatoms in the first and third positions of the ring, and two carbonyl groups in the second and fourth

# B. Ravali and A. Niranjana Kumar have equal contribution and both may be considered as first authors.

positions, respectively. Different replacements occur at the third and fifth locations, allowing for diverse changes to the molecule. TZD derivatives are important heterocyclic molecules with a variety of pharmacological actions, including. antitumor[19], antiarthritic[20], antihyperglycemic, anti-inflammatory[21], and antimicrobial[22], *etc*. TZD compounds can block specific enzymes as aldose reductase, phosphoinositide-3-kinase, Pim kinase, cyclooxygenase, D-glutamate ligase, and histone deacetylase[23,24].

On the other hand, among the leading classes of heterocycles that have drawn the greatest attention as pharmacophores in drug development during the past 20 years are 1,2,3-triazoles. The synthetic 1,2,3-triazoles exhibit a wide range of biological actions, including anticancer[25-27], antituberculosis, and antiviral properties[28] and recently introduced as potent α-glucosidase inhibitors[29]. In addition to being synthetic, several semi-synthetic natural products 1,2,3-triazoles, have also been observed to exhibit distinct primary biological functions such as forskolin-1,2,3-triazoles[30], eugenol-1,2,3-triazoles[31], andrographolide-1,2,3-triazoles[32], indole-1,2,3-triazoles[33], *etc*.

Recently, vanillin-1,2,3-triazole fragments also reported with their antifungal activities[34]. To the best of my knowledge, no derivatives have been documented with a combination of these three active pharmacophores. Viewing the importance of these three active pharmacophores (vanillin, 2,4-thiazolidinedione and 1,2,3-triazoles), we synthesized a series of vanillin-TZD-triazole hybrid derivatives and the evaluation of their anti-cancer and *in silico* docking studies of the active molecules is reported.

Chemistry

The four-step synthesis to obtain the target molecules is depicted in Scheme 1. In the first step, the precursor benzylated vanillins **2a-d** were synthesized by treating vanillin **1** with substituted benzyl bromides/chlorides/K_2CO_3 in DMF (90-95% yiespectrald). In the second step, compounds **4a-d** were prepared by attempting Knoevenagel condensation reaction between benzylated vanillins **2a-d** and 2,4-thiazolidinedione **3** under reflux conditions in the presence of piperidine as catalyst. In the third step, compounds **4a-d** were condensed with propargyl bromide in the presence of K_2CO_3 in dry dimethyl formamide at RT for 4 hr to obtain propargylated compounds **5a-d**. In the final step, the terminal alkynes

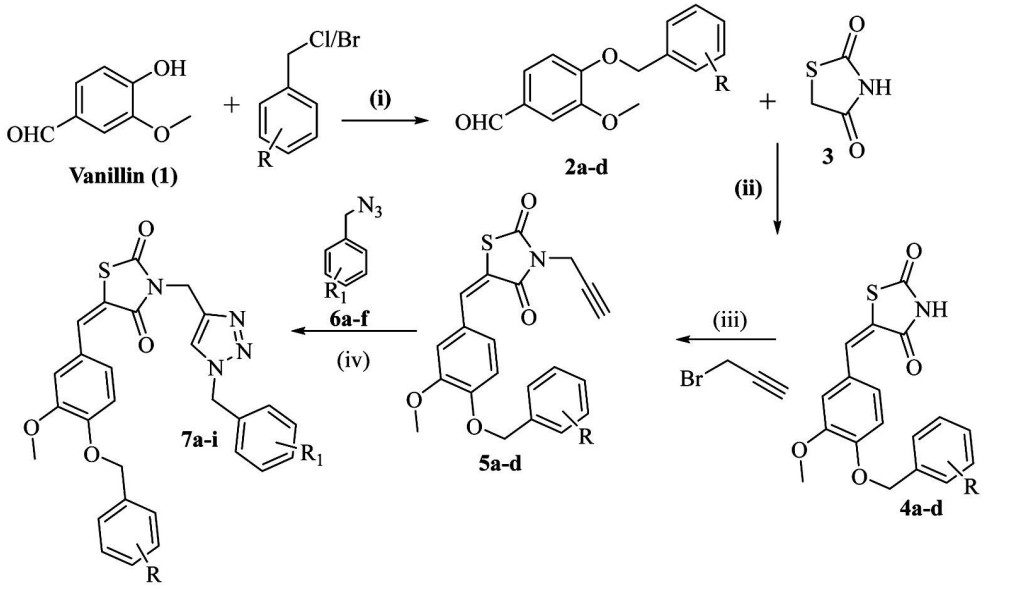

Where R and R_1 =

7a: R = 3-Cl; R_1 = 4-H
7b: R = 3-Cl; R_1 = 4-Cl
7c: R = 3-Cl; R_1 = 4-Br
7d: R = 3-Cl; R_1 = 4-F
7e: R = 3-Cl; R_1 = 3-Cl
7f: R = 4-Br; R_1 = 4-F
7g: R = 4-Cl; R_1 = 4-F
7h: R = 4-Cl; R_1 = 4-Br
7i: R = 4-F; R_1 = 4-F
7j: R = 4-F; R_1 = 4-Cl

Reagents and conditions:

(i) & (iii). K_2CO_3, DMF, RT 4 hr; (ii). Piperidine, Toluene, Reflux, 4 hr; (iv) CuI, THF, RT, Over night

Scheme 1 — Synthesis of vanilli-2,4-thiazolidinedione-1,2,3-troazoles **7a-j**

5a-d and various substituted azides **6a-f** (synthesized *in situ* from their halides precursors)[35] were condensed under click chemistry reaction conditions in presence of copper iodide and dry tetrahydrofuran (THF) at RT for over-night to result in novel Vanilli-2,4-thiazolidinedione-1,2,3-troazoles (**7a-i**) in quantitative yields. All the synthesized derivatives were characterized by ^{1}H, ^{13}C NMR. IR and LC-MS spectra.

In vitro cytotoxic activity

All the compounds evaluated for *in vitro* cytotoxic activities against four cancer cell lines, like MDA-MB 231 (a Model late-stage breast cancer), MCF-7 (Brea0073t cancer), A549 (lung cancer) and FaDU (Hypopharyngeal carcinoma) using MTT assay. Doxorubicin was used as a standard (Table 1).

Among all the synthesized derivatives, **7f** (*p*-bromo and *p*-flouro substituted on phenyl) possessed excellent cytotoxicity (50.61%; IC_{30}: 21.98 μm) inhibition against MDA-MB 231 cell line compare to standard Doxorubicin (73.88%) and rest of the tested cell lines (MCF-7: 34.70%, A549: 22.26% and FaDU: 41.38%) displayed moderate cytotoxicity compare to standard Doxorubicin (69.07%, 59.97% and 64.23% respectively). The one more derivative **7i** (*p*- fluro substituted on both phenyls) also significantly inhibited against FaDU cell line (52.08%; IC_{30}: 23.57 μm) compared to standard Doxorubicin (64.23%) and moderately inhibited reaming three cell lines (FaDU: 16.53%, MCF-7: 39.96%% and A549: 40.13%) compared to standard (73.88%, 69.07%, and 59.97% respectively).

In silico Molecular Docking Studies

Molecular docking is an indispensable computational tool in the field of drug development. The purpose is to evaluate the therapeutic potential of chemical compounds and determine their binding affinity, interaction, and stability in the protein-ligand complex. Within bonding interactions, the presence of ionic, hydrogen, Van der Waals, and hydrophobic interactions is commonly observed. It is usually recognized that molecular recognition heavily depends on these interactions. In this study, synthesized compounds were docked with succinate dehydrogenase, a key metabolic enzyme involved in cellular metabolism, specifically in the tricarboxylic acid (TCA) cycle and the electron transport chain (ETC). While SDH has traditionally been associated with energy production, its role in cancer cell survival and proliferation has drawn more attention, particularly in the context of certain genetic mutations linked to hereditary cancers[36]. The compounds exhibited higher binding affinity in comparison to the established inhibitor, malonate. Binding energy and pocket for each ligand with SDH protein are summarized in Table 2.

The BCL-2 family has a vital function in controlling apoptosis, a highly coordinated process of programmed cell death that is essential for maintaining tissue homeostasis. The family consists of both anti-apoptotic and pro-apoptotic proteins that interact to regulate the intrinsic or mitochondrial pathway of apoptosis. Aberrant regulation of the BCL-2 family is a prevalent characteristic in cancer, leading to enhanced cell viability, resistance to programmed cell death, and the development of cancer[37]. Pro-apoptotic factors are prevented from being activated by members such as BCL-2, BCL-XL, BCL-W, and MCL-1, resulting in the inhibition of apoptosis in breast[38] and hypo-pharyngeal cancer[39]. Therefore, a molecular docking analysis was conducted to assess the binding affinity of

Table 1 — Cytotoxic potential of vanillin conjugates against various human cancer cell lines by MTT assay

Compd	Growth inhibition in different human cancer cell lines, 10 μM, 48 h (in%)			
	MDAMB 231	MCF-7	A549	FaDU
7a	43.55	0.32	21.68	37.77
7b	40.41	42.96	22.72	34.37
7c	26.10	23.97	28.62	23.71
7d	27.13	23.02	22.44	34.45
7e	16.77	11.96	31.05	30.81
7f	50.61	34.70	22.26	41.38
7g	22.11	23.19	19.14	23.71
7h	27.27	36.80	27.58	33.75
7i	16.53	39.96	40.13	52.08
7j	18.11	36.71	16.13	38.36
Doxorubicin	73.88	69.07	59.97	64.23

Table 2 — Represents predicted physico-chemical properties and drug-likeness nature of compounds

Druglikeness Parameters	**7f**	**7i**
MW	608.05	548.571
HBD	0	0
HBA	8	8
Molar refractivity	152.40	144.71
log P	5.398	5.42
Lipinski rule	NO	NO
Verber rule	YES	YES
Ghose rule	NO	NO
Egan rule	YES	YES
Muegge rule	NO	NO

7f, 7i, and various established inhibitors towards the target proteins BCL-2, BCL-XL, BCL-W, and MCL-1. Throughout the analysis, it was discovered that both **7f** and **7i** had an exceptional affinity for all receptor proteins, as evidenced by their high binding energy (Table 3). **7f** and **7i** had the highest binding energy (–17.8 and –17.7, respectively) compared to BCL-W, and their all interacting amino acid residues matched with the inhibitor amino acid residues (Fig. 1).

The drug-likeness analysis indicates that the compound is not compliant with the Lipinski, Ghose, and Muegge rules, but it follows the Verber and Egan rules Table 2. The interpretation of the ADMET results involves assessing the significance of their marginal value concerning their final value. When considering the absorption section, it is crucial to note that the Caco-2 permeability value should exceed -5.15, MDCK should be greater than 2×10^{-6}, and intestinal absorption must be higher than 30%. In the distribution section, human VDss is categorized as high when it exceeds 2.81 L/kg and low when it drops below 0.71 L/kg. It is believed that compounds can pass the blood-brain barrier if their BBB permeability logBB value is greater than 0.3, and that compounds

Table 3 — Represents the binding energy, inhibition constant, and binding site of ligand **7f** and **7i** with different receptor proteins

Receptor (PDB ID)	Ligand	Binding energy (Kcal/mol)	Ki (μM)	BINDING POCKETS	H-bond (Å)
SDH (6VAX)	**7f**	–16.7	5.61485×10^{-13}	ASN110, ARG69, GLU73, ARG97, PHE94, GLN56, ARG58, TRP55, PRO54, GLU111, PRO53	GLN56 (3.9), ARG69 (5.1)
	7i	–16.5	7.87141×10^{-13}	PRO53, PRO54, GLU111, ARG58, PHE94, ARG97, GLU73, TRP55, GLN56, ARG69, ASN110	GLU73 (5.8), ARG69 (5.1), GLN56 (3.9), GLU111 (5.6)
	Malonate	–4.8	3.01198×10^{-4}	GLU564, ARG507, ARG512, LEU158, LYS550, GLU159, THR508, ASP561, SER509	SER509 (3.4), THR508 (3.4), LEU158 (3.6), ARG512 (4.8)
BCL-2 (1G5M)	**7f**	–13.7	8.91365×10^{-11}	GLY194, GLN190, ILE189, TRP195, ASN11, TYR9, ARG6, THR7, GLY8, HIS186, ASN182	ASN11(3.8), THR7 (4.6)
	7i	–13.7	8.91365×10^{-11}	THR7, GLY8, TYR9, TRP195, ASP196, ASN11, HIS186, ILE189, ASN182, GLY194	THR7 (3.6), TRP195 (4.7)
	Venetoclax	–10.4	2.3488×10^{-8}	ARG12, ASP35, VAL36, THR41, GLU38, SER49, LYS17, HIS94, THR47, GLU45, ASP10, GLU48, GLY46, THR7, GLY8, GLU13, TYR9	GLY8 (3), ASP10 (4.7), GLU45 (4.9), LYS17 (5.4) (5.9)
BCL-XL (1R2D)	**7f**	–16.2	1.30654×10^{-12}	ALA93, VAL141, GLU96, GLY138, TYR101, TYR195, PHE97	–
	7i	–16.9	4.00519×10^{-13}	TYR101, TYR195, VAL141, GLY138, ALA93, PHE97, GLU96	–
	A-1331852	–15.3	5.97502×10^{-12}	TYR195, ARG139, ASN136, GLY138, LEU130, GLU129, ARG132, SER106, SER145, PHE146, THR109, ASP107, ALA149, ARG102, LEU108, PHE105, ALA142, PHE97, VAL141, TYR101, ALA93, GLU96	ASN136 (4.7), ARG139 (3.6), SER106 (4.5)
BCL-W (1MK3)	**7f**	–17.8	8.75806×10^{-14}	TRP143, LEU129, LEU133, PHE98, LEU95, PHE86, ILE137, ASN91, GLU145, GLY142	–
	7i	–17.7	1.03697×10^{-13}	PHE98, TRP143, LEU133, LEU129, PHE86, ILE137, LEU95, GLU145, ASN91	–
	Navitoclax	–12	1.57445×10^{-9}	ASP83, PHE86, ARG94, LEU133, ASN91, TRP92, GLU145, SER139, ILE137, SER140, TRP136, LEU95, PRO90, LEU129, PHE98, TRP143	SER140 (2.7), SER139 (3.8)
MCL-1 (2MHS)	**7f**	–11.8	2.20721×10^{-9}	PHE149, HIS159, PHE150, VAL51, THR97, ARG94, GLY93, ASN91	–
	7i	–11.9	1.86417×10^{-9}	GLN140, GLY88, PHE85, LYS133, TRP136, TRR90, ARG94, ILE95, TRP92	–
	AZD5991	–9	2.49946×10^{-7}	TRP136, HIS162, GLY158, GLY145, GLU148, ARG141, LYS139, HIS160, GLN140, TRP92, HIS162, TRP136, TRP92 (5.4), GLN140 (3.1)	TRP92 (5.4), GLN140 (3.1)

Table 4 — Represents calculated Adsorption, Distribution, Metabolism, Excretion and Toxicity (ADMET) parameters of ligands

Compd	Adsorption			Distribution			Metabolism	Excretion		Toxicity		
	Caco2 (log cm/s)	MDCK (cm/s)	Intestinal absorption (%)	BBB (log BB)	CNS (log PS)	VD (log L/kg)	CYP2D6/ CYP1A2 inhibitor	CL (mL/ min/kg)	T1/2 (min)	AMES toxicity	hERG Blockers	Skin Sensitisation
	Permeability			Permeability								
7f	–4.766	2.5×10^{-5}	91.906	–1.532	–3.049	–0.403	NO	5.496	0.014	NO	NO	NO
7i	–4.724	2.7×10^{-5}	93.041	–1.556	–3.21	–0.582	NO	9.801	0.013	NO	NO	NO

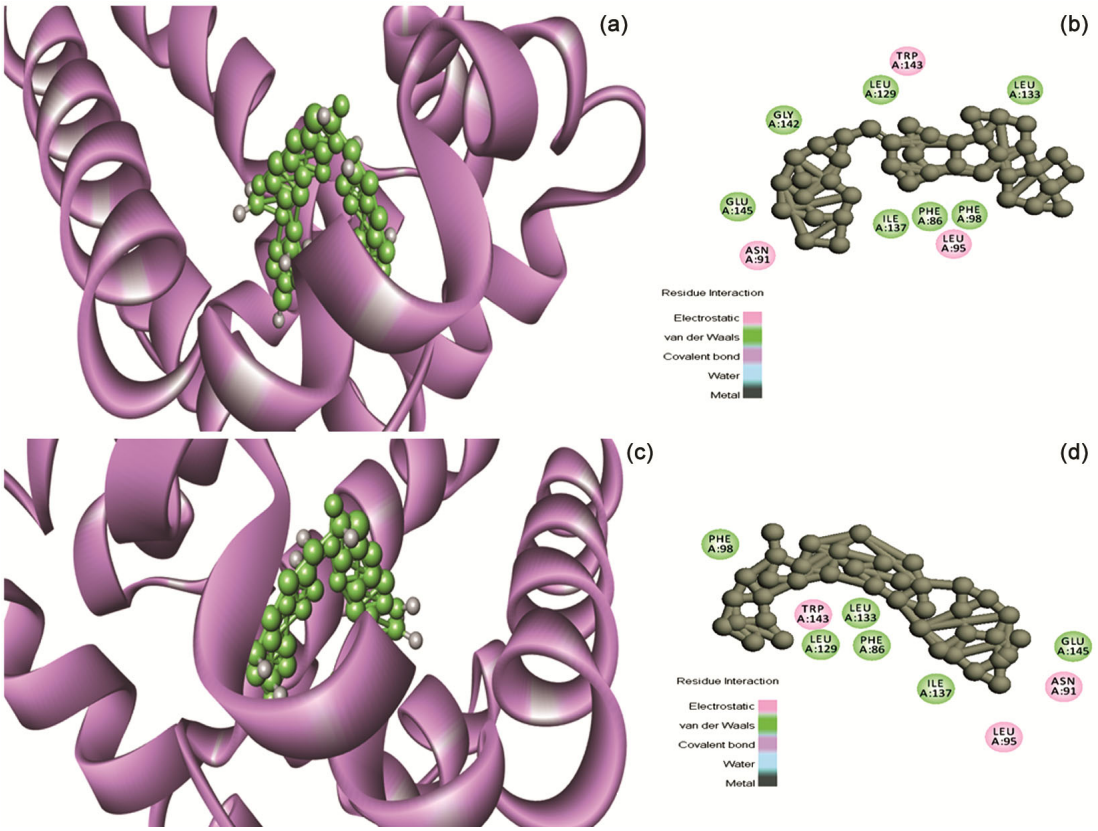

Fig. 1 — Binding interaction of **7f** and **7i** with BCL-W protein: (**A**) 3D representation of binding pocket of **7f**, **(B**) 2D representation of binding pocket of **7f**, (**C**) 3D representation of binding pocket of **7i**, (**D**) 2D representation of binding pocket of **7i**

with a logBB value below -1 have poor distribution across the barrier. The permeability of the central nervous system (CNS) is determined by the logPS value. A logPS value above -2 suggests that a substance can penetrate the CNS, while a logPS value below -3 suggests the contrary. The liver enzyme known as Cytochrome P450s is essential for drug metabolism in the body. CYP2D6 and CYP1A2 are significant subtypes of cytochrome P450 enzymes that have a pivotal role in determining the metabolic fate of a molecule. In the excretion section, a clearance value greater than 5 is considered excellent, while a clearance value less than 5 indicates inadequate drug elimination. The drug has a half-life ranging from 0 to 0.7. In the toxicity parts, none of the compounds showed hERG. Blocker capability, skin sensitization, or AMES toxicity (Table 4).

Experimental Section

Chemistry

Melting points of all the compounds were recorded on Casia-Siamia (VMP-AM) melting point apparatus and uncorrected. IR spectra were recorded on a Perkin–Elmer FT-IR 240-C spectrometer using KBr optics. NMR spectra were recorded on Burker Avance 500 MHz in $CDCl_3$ and DMSO-d_6 using TMS as internal standard. Electron impact (EI) and chemical ionization mass spectra were recorded on a VG Micro mass model 7070H instrument. All the reactions were monitored on silica gel percolated TLC plates of Merck and spots

were visualized with UV light. Silica gel (100-200 mesh) used for column chromatography was procured from Merck.

General procedure and spectral data of synthesized compounds

Synthetic procedures for benzylation of Vanillin, 2a-d

Vanillin **1** (1.0 g., 6.578 mmol) along with potassium carbonate (1.361 g., 9.862 mmol) was dissolved in 20 mL of dry dimethyl formamide and later substituted benzyl chloride\bromide (1.5 mL) was added slowly while stirring. The reaction mixture was stirred for 4 hr at RT to afford crude benzylated derivatives. Later, the reaction mixture was poured into a distilled water (500 mL) slowly while stirring then filtered to obtain substituted vanillin benzylated derivatives **2a-d**.

4-((3-Chlorobenzyl)oxy)-3-methoxybenzaldehyde, 2a: Colorless solid. Yield 92%. m.p. 55-57°C. IR (KBr): 2927, 1681, 1585, 1508, 1423, 1272, 1130, 999, 867, 666 cm^{-1}; ^1H NMR ($CDCl_3$, 400 MHz): δ 9.85 (s, 1H), 7.44 (m, 3H), 7.39 (m, 3H), 6.97 (d, *J* = 8.2 Hz, 1H), 5.20 (s, 2H), 3.95 (s, 3H); ^{13}C NMR ($CDCl_3$, 75 Hz): δ 56.07, 70.09, 109.54, 112.48, 125.23, 126.47, 126.65, 127.29, 128.42, 128.56, 130.00, 130.04, 130.60, 150.12, 153.26, 190.89.

4-((4-Bromobenzyl)oxy)-3-methoxybenzaldehyde, 2b: Colorless solid. Yield 95%. m.p. 79-81°C. ^1H NMR ($CDCl_3$, 400 MHz): δ 9.85 (s, 1H), 7.51 (t, *J* = 5.4 Hz, 2H), 7.44 (m, 1H), 7.31 (d, *J* = 8.4 Hz, 1H), 6.96 (d, *J* = 8.2 Hz, 3H), 5.18 (s, 2H), 3.95 (s, 3H); HR-MS: *m/z* 321 (M^+). Obsd. for $C_{15}H_{13}BrO_3$.

4-((4-Chlorobenzyl)oxy)-3-methoxybenzaldehyde, 2c: Colorless solid. Yield 90%. m.p. 69-71°C. ^1H NMR ($CDCl_3$, 400 MHz): δ 9.84 (s, 1H), 7.43 (d, *J* = 1.8 Hz, 1H), 7.41 (m, 3H), 7.37 (d, *J* = 2.6 Hz, 2H), 6.95 (s, 1H), 5.20 (s, 2H), 3.94 (s, 3H); ^{13}C NMR ($CDCl_3$, 75 Hz): δ 56.06, 70.14, 109.50, 112.46, 126.47, 128.61, 128.94, 130.54, 134.09, 134.54, 150.12, 153.31, 190.87; HR-MS: *m/z* 277 ($M+1^+$). Obsd. for $C_{15}H_{13}ClO_3$.

Synthesis of substituted (E)-5-(4-(benzyloxy)-3-methoxybenzylidene)thiazolidine-2,4-diones 4a-d general procedure

A mixture of thiazolidine-2,4-dione **3** (0.6 g., 5.128 mmol) and compounds **2a-d** (1 eq) and with catalytic quantity of piperidine was refluxed in toluene with continuous removal of water using dean stark apparatus for 4 h. The reaction mixture was cooled to 25°C to obtain a pale yellow solid. The solid was filtered off and washed with water followed by minimal amount of methanol yielded pure compounds **4a-d**.

(E)-5-(4-((4-Chlorobenzyl)oxy)-3-methoxybenzylidene)thiazolidine-2,4-dione, 4b: Pale yellow solid. Yield 95%. m.p. 217-219°C. IR (KBr): 3039, 1731, 1685, 1589, 1508, 1465, 1334, 1265, 1145, 1091, 1002, 871 cm^{-1}; ^1H NMR (400 MHz, DMSO-d_6): δ 12.52 (s, 1H), 7.75 (s, 1H), 7.48 (m, 10H), 7.18 (ddd, *J* = 10.3, 8.1, 1.8 Hz, 1H), 5.18 (s, 2H), 3.83 (s, 3H); ^{13}C NMR (DMSO-d_6, 75 Hz): δ 56.12, 69.52, 114.09, 114.14, 121.25, 123.95, 126.63, 128.42, 128.97, 130.13, 132.54, 133.08, 136.09, 149.71, 150.01, 167.87, 168.43; HR-MS: *m/z* 376 ($M+1^+$). Obsd. for $C_{18}H_{14}ClNO_4S$.

(E)-5-(4-((4-Bromobenzyl)oxy)-3-methoxybenzylidene)thiazolidine-2,4-dione, 4c: Pale yellow solid. Yield 96%. ^1H NMR (400 MHz, DMSO-d_6): δ 12.52 (s, 1H), 7.75 (s, 1H), 7.62 (m, 3H), 7.42 (d, *J* = 8.4 Hz, 3H), 7.23 (m, 1H), 5.17 (s, 2H), 3.83 (s, 3H); ^{13}C NMR (DMSO-d_6, 75 Hz): δ 56.13, 69.55, 114.10, 114.15, 121.25, 123.95, 126.63, 130.43, 131.89, 132.54, 136.52, 149.71, 150.00, 167.86, 168.42.

Procedure for propargylation of 4a-d

Compounds **4a-d** (0.5 g., 1 eq) along with potassium carbonate (1.5 eq) was dissolved in 10 mL of dry dimethyl foramamide and later propargyl bromide (1.0 mL) was added slowly while stirring. The reaction mixture was stirred for 4 h at RT. This crude residue was poured in water (500 mL) slowly while stirring, then filtered washed with water and dried to get pure propargylated derivatives **5a-d** in pure state.

(E)-5-(4-((3-Chlorobenzyl)oxy)-3-methoxybenzylidene)-3-(prop-2-yn-1-yl)thiazolidine-2,4-dione, 5a: Colorless solid. Yield 91%. IR (KBr): 3274, 3020, 2129, 1739, 1681, 1596, 1508, 1380, 1334, 1265, 1145, 1083, 999 cm^{-1}; ^1H NMR (400 MHz, $CDCl_3$): δ 7.87 (s, 1H), 7.83 (s, 1H), 7.44 (s, 1H), 7.38 (d, *J* = 8.5 Hz, 1H), 7.31 (m, 2H), 7.07 (m, 2H), 6.93 (dd, *J* = 8.4, 5.8 Hz, 1H), 5.30 (s, 1H), 5.20 (s, 1H), 4.85 (s, 1H), 3.95 (t, *J* = 5.4 Hz, 3H), 3.49 (s, 1H); ^{13}C NMR ($CDCl_3$, 75 Hz): δ 31.07, 44.56, 56.14, 70.44, 72.40, 113.03, 113.67, 124.53, 125.22, 127.28, 128.39, 128.93, 130.03, 130.35, 134.29, 134.63, 138.29, 149.94, 150.21, 165.53, 167.78.

(E)-5-(4-((4-Bromobenzyl)oxy)-3-methoxybenzylidene)-3-(prop-2-yn-1-yl)thiazolidine-2,4-dione, 5b: ^{13}C NMR ($CDCl_3$, 75 Hz): δ 30.64, 56.05, 70.20, 72.15, 77.34, 113.02, 113.66, 118.51, 122.17, 124.53, 126.57, 128.89, 131.89, 134.62, 135.24, 149.93, 150.23, 165.16, 166.83; HR-MS: *m/z* 458 (M^+). Obsd. for $C_{21}H_{16}BrNO_4S$.

(E)-5-(4-((4-Chlorobenzyl)oxy)-3-methoxybenzylidene)-3-(prop-2-yn-1-yl)thiazolidine-2,4-dione, 5c: Colorless solid. Yield 91%. ^{1}H NMR (400 MHz, $CDCl_3$): δ 7.87 (s, 1H), 7.42 – 7.31 (m, 3H), 7.26 (s, 1H), 7.08 (m, 2H), 6.93 (d, *J* = 8.4 Hz, 1H), 5.17 (s, 2H), 4.50 (d, *J* = 2.5 Hz, 2H), 3.93 (s, 3H), 2.27 (t, *J* = 2.5 Hz, 1H); ^{13}C NMR ($CDCl_3$, 75 Hz): δ 30.64, 56.05, 70.17, 72.15, 113.02, 113.66, 118.49, 124.54, 126.55, 128.60, 128.93, 134.06, 134.71, 149.94, 150.26, 165.16, 166.86; HR-MS: *m/z* 414 ($M+1^+$). Obsd. for $C_{21}H_{16}ClNO_4S$.

Procedure for synthesis of Vanillin-2,4 thiazolidinedione-1,2,3-triazoles, 7a-i

Intermediates **5a-d** (0.5 g., 1.0 eq) was dissolved in dry THF (30 mL) and catalytic amount of copper iodide was added. To this substituted aromatic azide (**6a-f**) (1.5 eq) in dry THF were added slowly while stirring at RT under nitrogen atmosphere for 12 h. Later, the solvent was removed under reduced pressure and the residue was diluted with distilled water and extracted thrice with dichloromethane. The combined organic layers were dried over anhydrous Na_2SO_4 and concentrated to get the product crude **7a-i**. These crude products are further purified by column chromatography with hexane and mixture of ethyl acetate in hexane to get pure Vanillin-2,4 thiazolidinedione-1,2,3-triazoles (**7a-i**) in quantitative yields.

(E)-3-((1-Benzyl-1*H*-1,2,3-triazol-4-yl)methyl)-5-(4-((4-chlorobenzyl)oxy)-3-methoxybenzylidene)-thiazolidine-2,4-dione, 7a: Coloeless solid. Yield 80%. IR (KBr): 3124, 3078, 2364, 1743, 1689, 1585, 1512, 1461, 1380, 1257, 1145, 1083, 995 cm^{-1}; ^{1}H NMR (400 MHz, DMSO-d_6): δ 7.83 (s, 1H), 7.52 (s, 1H), 7.44 (s, 1H), 7.44 (m, 2H), 7.31 (d, *J* = 1.0 Hz, 3H), 7.26 (s, 2H), 7.06 (m, 2H), 6.91 (d, *J* = 8.4 Hz, 1H), 5.49 (s, 2H), 5.30 (s, 3H), 5.17 (s, 2H), 3.93 (s, 3H); HR-MS: *m/z* 616 ($M+1^+$). Obsd. for $C_{28}H_{21}Cl_3N_4O_4S$.

(E)-3-((1-(4-Chlorobenzyl)-1*H*-1,2,3-triazol-4-yl)methyl)-5-(4-((3-chlorobenzyl)oxy)-3-methoxybenzylidene)thiazolidine-2,4-dione, 7b: Coloeless solid. Yield 82%. IR (KBr): 3116, 3074, 2364, 1743, 1685, 1589, 1515, 1384, 1315, 1265, 1141, 999, 786 cm^{-1}; ^{1}H NMR (500 MHz, DMSO-d_6): δ 8.19 (s, 1H), 7.93 (d, *J* = 8.9 Hz, 1H), 7.53 (s, 1H), 7.46 (m, 4H), 7.35 (m, 2H), 7.28 (s, 2H), 7.22 (m, 2H), 5.58 (s, 2H), 5.19 (m, 2H), 4.89 (d, *J* = 14.7 Hz, 2H), 3.84 (t, *J* = 11.2 Hz, 3H); ^{13}C NMR (DMSO-d_6, 75 Hz): δ 40.08, 51.98, 55.66, 68.96, 113.39, 118.33, 123.73, 126.04, 126.37, 127.50, 127.95, 128.74, 129.31, 129.95, 130.44, 132.85, 133.09, 133.60, 134.89, 139.09, 141.45, 149.22, 149.27, 159.85, 165.18, 166.98; HR-MS: *m/z* 582 ($M+1^+$). Obsd. for $C_{28}H_{22}Cl_2N_4O_4S$.

(E)-3-((1-(4-Bromobenzyl)-1*H*-1,2,3-triazol-4-yl)methyl)-5-(4-((3-chlorobenzyl)oxy)-3-methoxybenzylidene)thiazolidine-2,4-dione, 7c: Coloeless solid. Yield 76%. ^{1}H NMR (500 MHz, DMSO-d_6): δ 8.18 (s, 1H), 7.92 (d, *J* = 9.2 Hz, 1H), 7.60 (m, 2H), 7.53 (s, 2H), 7.44 (m, 3H), 7.28 (dd, *J* = 6.6, 1.8 Hz, 1H), 7.28 (m, 2H), 7.13 (d, *J* = 8.5 Hz, 1H), 5.60 (d, *J* = 33.0 Hz, 2H), 5.21 (d, *J* = 1.6 Hz, 2H), 4.88 (d, *J* = 14.9 Hz, 2H), 3.85 (d, *J* = 1.8 Hz, 3H); ^{13}C NMR (DMSO-d_6, 75 Hz): δ 52.06, 52.56, 55.67, 68.97, 113.66, 113.81, 118.08, 118.32, 121.30, 123.75, 126.38, 127.51, 127.96, 129.62, 130.27, 130.45, 131.38, 131.71, 133.11, 133.79, 134.64, 135.31, 139.09, 141.44, 145.32, 149.23, 149.76, 165.19, 166.99; HR-MS: *m/z* 626 ($M+1^+$). Obsd. for $C_{28}H_{22}BrClN_4O_4S$.

(E)-5-(4-((3-Chlorobenzyl)oxy)-3-methoxybenzylidene)-3-((1-(4-fluorobenzyl)-1*H*-1,2,3-triazol-4-yl)methyl)thiazolidine-2,4-dione, 7d: Coloeless solid. Yield 79%. IR (KBr): 3074, 2927, 2360, 1739, 1685, 1593, 1512, 1380, 1269, 1141, 1087, 786 cm^{-1}; ^{1}H NMR (500 MHz, DMSO-d_6): δ 8.18 (s, 1H), 7.93 (d, *J* = 8.5 Hz, 2H), 7.53 (s, 2H), 7.53 (m, 4H), 7.28 (m, 4H), 5.56 (s, 2H), 5.19 (d, *J* = 17.6 Hz, 2H), 4.87 (d, *J* = 14.5 Hz, 2H), 3.85 (d, *J* = 1.6 Hz, 3H); HR-MS: *m/z* 566 ($M+1^+$). Obsd. for $C_{28}H_{22}ClFN_4O_4S$.

(E)-3-((1-(3-Chlorobenzyl)-1*H*-1,2,3-triazol-4-yl)-methyl)-5-(4-((3-chlorobenzyl)oxy)-3-methoxybenzylidene)thiazolidine-2,4-dione, 7e: Coloeless solid. Yield 80%. IR (KBr): 2927, 2858, 2364, 1735, 1685, 1589, 1512, 1423, 1377, 1272, 1146, 1087, 995, 779 cm^{-1}; ^{1}H NMR (500 MHz, DMSO-d_6): δ 8.21 (s, 1H), 7.93 (d, *J* = 8.1 Hz, 1H), 7.53 (s, 2H), 7.51 – 7.38 (m, 6H), 7.28 – 7.16 (m, 3H), 5.60 (s, 2H), 5.21 (s, 2H), 4.89 (d, *J* = 14.6 Hz, 2H), 3.85 (d, *J* = 1.6 Hz, 3H); ^{13}C NMR (DMSO-d_6, 75 Hz): δ 40.63, 52.53, 56.20, 69.51, 114.18, 114.34, 124.35, 126.58, 126.84, 127.21, 127.97, 128.43, 128.64, 130.92, 131.91,,

133.60, 133.74, 141.96, 165.64, 167.41; HR-MS: *m/z* 582 ($M+1^+$). Obsd. for $C_{28}H_{22}Cl_2N_4O_4S$.

(E)-5-(4-((4-Bromobenzyl)oxy)-3-methoxybenzy--lidene)-3-((1-(4-fluorobenzyl)-1*H*-1,2,3-triazol-4-yl)methyl)thiazolidine-2,4-dione, 7f: Coloeless solid. Yield 79%. IR (KBr): 2923, 2854, 2360, 1739, 1685, 1593, 1512, 1461, 1380, 1272, 1141, 1091, 1022 cm^{-1}; ^1H NMR (500 MHz, DMSO-d_6): δ 8.18 (s, 1H), 7.92 (s, 1H), 7.55 (ddt, *J* = 8.6, 5.6, 2.4 Hz, 5H), 7.29 (m, 5H), 5.76 (s, 1H), 5.56 (s, 2H), 5.17 (s, 2H), 4.90 (s, 2H), 3.83 (s, 3H); ^{13}C NMR (DMSO-d_6, 75 Hz): δ 40.51, 52.55, 56.14, 69.68, 114.23, 114.25, 115.71, 115.88, 118.69, 122.01, 124.23, 130.71, 130.75, 132.17, 141.78, 141.93, 149.66, 150.48, 165.67, 167.47; HR-MS: *m/z* 610 ($M+1^+$). Obsd. for $C_{28}H_{22}BrFN_4O_4S$.

(E)-5-(4-((4-Chlorobenzyl)oxy)-3-methoxybenzy-lidene)-3-((1-(4-fluorobenzyl)-1*H*-1,2,3-triazol-4-yl)methyl)thiazolidine-2,4-dione, 7g: Coloeless solid. Yield 82%. ^1H NMR (400 MHz, DMSO-d_6): δ 8.16 (s, 1H), 7.91 (d, *J* = 6.7 Hz, 1H), 7.47 (m, 7H), 7.23 (m, 3H), 5.56 (s, 2H), 5.19 (s, 2H), 4.89 (s, 2H), 3.83 (s, 3H); ^{13}C NMR (DMSO-d_6, 75 Hz): δ 41.82, 57.25, 60.91, 74.28, 118.92, 119.04, 120.71, 120.93, 123.51, 128.90, 131.23, 133.73, 134.90, 135.54, 135.62, 137.85, 140.81, 146.65, 154.49, 155.05, 164.34, 170.42; HR-MS: *m/z* 565 ($M+1^+$). Obsd. for $C_{28}H_{22}ClFN_4O_4S$.

(E)-3-((1-(4-Bromobenzyl)-1*H*-1,2,3-triazol-4-yl)-methyl)-5-(4-((4-chlorobenzyl)oxy)-3-methoxybenzylidene)thiazolidine-2,4-dione, 7h: Coloeless solid. Yield 78%. ^1H NMR (400 MHz, DMSO-d_6): δ 8.32 (s, 1H), 7.93 (s, 3H), 7.52 – 7.41 (m, 5H), 7.23 (dd, *J* = 22.1, 18.5 Hz, 4H), 5.64 (s, 2H), 5.20 (s, 2H), 4.87 (s, 2H), 3.84 (s, 3H); ^{13}C NMR (DMSO-d_6, 75 Hz): δ 40.62, 52.99, 56.19, 69.56, 114.23, 114.35, 118.55, 124.24, 126.47, 128.98, 129. 27, 129.81, 130.14, 133.10, 133.25, 134.29, 134.71, 136.07, 145.80, 149.73, 150.35, 165.63, 167.38; HR-MS: *m/z* 626 ($M+1^+$). Obsd. for $C_{28}H_{22}BrClN_4O_4S$.

(E)-3-((1-(4-Fluorobenzyl)-1*H*-1,2,3-triazol-4-yl)-methyl)-5-(4-((4-fluorobenzyl)oxy)-3-methoxy-benzylidene)thiazolidine-2,4-dione, 7i: Coloeless solid. Yield 80%. ^1H NMR (400 MHz, DMSO-d_6): δ 8.17 (s, 1H), 7.92 (s, 1H), 7.51 (dd, *J* = 8.6, 5.6 Hz, 2H), 7.39 (m, 3H), 7.26 (m, 6H), 5.76 (s, 1H), 5.56 (s, 2H), 5.17 (s, 2H), 4.89 (s, 2H), 3.83 (s, 3H); ^{13}C NMR (DMSO-d_6, 75 Hz): δ 52.50, 55.38, 56.15, 69.69, 114.20, 114.30, 115.71, 115.88, 115.99, 116.16, 118.79,124.07, 126.41, 130.64, 130.70, 130.79, 130.86, 134.14, 141.90, 149.74, 150.42, 152.97, 165.65, 167.47; HR-MS: *m/z* 549 ($M+1^+$). Obsd. for $C_{28}H_{22}F_2N_4O_4S$.

(E)-3-((1-(4-Chlorobenzyl)-1*H*-1,2,3-triazol-4-yl)-methyl)-5-(4-((4-fluorobenzyl)oxy)-3-methoxy-benzylidene)thiazolidine-2,4-dione, 7j: Coloeless solid. Yield 78%. IR (KBr): 2927, 2858, 2364, 1739, 1681, 1589, 1512, 1461, 1380, 1265, 1222, 1141, 1087, 1026 cm^{-1}; ^1H NMR (400 MHz, DMSO-d_6): δ 8.18 (s, 1H), 7.92 (d, *J* = 8.6 Hz, 1H), 7.52 (dd, *J* = 8.5, 5.7 Hz, 3H), 7.51 (m, 2H), 7.34 (d, *J* = 8.4 Hz, 2H), 7.23 (m, 3H), 5.74 (d, *J* = 19.9 Hz, 1H), 5.58 (s, 2H), 5.17 (s, 2H), 4.88 (d, *J* = 14.8 Hz, 2H), 3.83 (d, *J* = 1.6 Hz, 3H); ^{13}C NMR (DMSO-d_6, 75 Hz): δ 52.50, 53.06, 56.15, 69.70, 114.29, 115.71, 115.88, 124.21, 126.41, 129.24, 129.27, 129.81, 130.44, 130.63, 130.70, 133.25, 134.68, 135.38, 141.63, 150.43, 165.64, 167.48; HR-MS: *m/z* 566 ($M+1^+$). Obsd. for $C_{28}H_{22}ClFN_4O_4S$.

In vitro cytotoxic activity

Cell Culture

The MDAMB-231, A549, FaDU, and MCF-7 cell lines were cultivated in RPMI medium containing 10% Fetal Bovine Serum (FBS) and supplemented with a 1% penicillin-streptomycin mixture. The cells were incubated 24 hours until they reached a confluence of over 80-90%. This incubation was carried out in a humidified environment with 5% CO_2 at a temperature of 37°C.

In vitro cell cytotoxicity studies

To assess cytotoxicity, we employed the 3-(4,5-Dimethylthiazol-2-yl)-2,5-diphenyltetrazolium bromide (MTT) assay, which involved the compound **7i**. Initially, MDAMB-231, FaDU, MCF-7, and A549 cell lines were seeded into 96-well plates at a density of 5×10^3 cells per well, along with RPMI medium containing 10% Fetal Bovine Serum (FBS). Following an overnight incubation, the culture medium was replaced with fresh medium devoid of FBS, and this medium contained compound includes **7i**. After a post-treatment incubation period, the culture medium was removed, and 20 µL of MTT solution was added to each well, followed by a 4-hour incubation in an incubator. Once the incubation was completed, the MTT solution was aspirated from the 96-well plates. Subsequently, 150 µL of dimethyl

sulfoxide (DMSO) was added to each well to dissolve the purple formazan crystals generated from the MTT. Finally, the absorbance of the 96-well plates was measured at 570 nm using a microplate reader (Envision Multimode Plate Reader-Perkin Elmer, U.S.A.), and the inhibitory concentration (IC_{50} values) was determined.

In silico molecular Docking Studies

Preparation of Receptor

The 3D crystal structures of receptor protein succinate dehydrogenase (6VAX), BCL-2 (1G5M), BCL-XL (1R2D), BCL-W (1MK3), MCL-1 (2MHS) have been acquired from the RCSB Protein Data Bank. The PDB files obtained were processed using the BIOVIA Discovery Studio 3.5 software to eliminate ligands, water molecules, and unwanted heteroatoms that could potentially hinder the docking study. The protein molecules missing residues were repaired using AutoDock tools[40]. Further polar hydrogen atoms were included to enhance the stability of the binding complexes.

Preparation of Ligand

The chemical structure of the synthesized compounds was depicted using ACD/ChemSketch software. The designed structure was saved in the MDL Molfile format[27]. The inhibitors 3D structures have been retrieved from the PubChem database in SDF file format[27]. To facilitate further studies, the compounds and inhibitors MDL Molfile and SDF file were converted into the PDB file using the PyMOL Molecular Graphics System, Version 1.5.0.4 Schrodinger, LLC, USA.

Molecular docking

The interactions between receptor molecules and ligands were investigated using PyRx's AutoDock (V. 4.0) interface. The process started with the preparation of a receptor protein, which involved the simultaneous removal of surrounding water and addition of polar hydrogen molecules and Kollman charges. Once the rotatable bonds in each ligand were allowed to rotate, the Gasteiger charges were calculated. Each ligand was manually uploaded into the software. Every ligand is subjected to energy minimization before automatically being converted into the PDBQT format. Another step in the virtual screening process is to set up the grid box for the intended docking spot[41]. A grid box was utilized to create a grid map using AutoGrid**.** Following the establishment of a grid box encompassing the binding sites of the receptors, a rigid-flexible docking procedure was conducted. Throughout the docking process, a total of ten conformations were produced. The conformation with the most negative binding energy and RMSD values below 1.0Å was chosen and subsequently, the inhibition constant (Ki) was calculated. To examine the binding pocket and ligand poses, the interactions between the targeted receptor and the ligand were analyzed using BIOVIA Discovery Studio 3.5. This analysis revealed the specific locations of the binding sites and the various types of interactions between the desired protein and the docked ligand.

Drug-likeliness and ADMET prediction

Assessing drug-likeness and ADMET (absorption, distribution, metabolism, excretion, and toxicity) properties is crucial in drug discovery to evaluate a compound's safety and oral bioavailability. Key physicochemical attributes such as molecular weight (MW), topological polar surface area (TPSA), log P, molar refractivity, rotatable bonds, and hydrogen bond donors/acceptors influence pharmacokinetics. The pkCSM software was used to assess compounds based on Lipinski's Rule of Five, Ghose's Rule[42], Veber's Rule[43], Egan's Rule[44], and Muegge's Rule[45]. Lipinski's rule suggests MW <500 Da, log P <5, ≤5 hydrogen bond donors, and ≤10 hydrogen bond acceptors. Ghose's rule refines these parameters to MW 160–480, log P 0.4–5.6, molar refractivity 40–130, and an atom count of 20–70. Veber's criteria prioritize ≤10 rotatable bonds and PSA ≤140 Å², while Egan's rule limits TPSA to ≤132 Å² and log P to ≤6. Muegge's rule expands these by suggesting MW 200–600, log P -2 to 5, PSA ≤150 Å², ≤7 rings, and ≤15 rotatable bonds.

The ADMET filter was applied to identify compounds with favorable pharmacokinetics and minimal toxicity[46]. Absorption governs drug entry into systemic circulation, distribution determines its spread in tissues, metabolism involves biochemical modifications, and excretion eliminates drugs and metabolites. This screening ensures the selection of promising drug candidates for further development.

Acknowledgements

The authors thank the Director CSIR-CIMAP, Lucknow, for his constant encouragement and support. Author Akanksha Singh is thankful to

Academy of Scientific and Innovative Research (AcSIR), Ghaziabad, Uttar Pradesh, India for providing financial assistance.

References

1 Zhang S & Mueller C, *J Agric Food Chem*, 60 (2012) 10433.
2 Bezerra D P, Soares A K N & De Sousa D P, *Oxid Med Cell Longev*, 2016 (2016) Article ID 9734816, (http://dx.doi.org/10.1155/2016/9734816).
3 Banerjee G & Chattopadhyay P, *J Sci Food Agric*, 99 (2019) 499.
4 Ciriminna R, Fidalgo A, Meneguzzo F, Parrino F, Ilharco L M & Pagliaro M, *Chem Open*, 8 (2019) 660.
5 Ma W, Li X, Song P, Zhang Q, Wu Z, Wang J, Li X, Xu R, Zhao W, Liu Y, Liu H, Yao X, Tang X & Chen P, *Eur J Pharm*, 849 (2019) 43.
6 Kim H J, Hwang I K & Won M H, *Brain Res*, 1181 (2007) 130.
7 Abraham D J, Mehanna A S, Wireko F C, Whitney J, Thomas R P & Orringer E P, *Blood*, 77 (1991) 1334.
8 Tai A, Sawano T & Yazama F, *Biosci Biotech Biochem*, 75 (2011) 2346.
9 Lim E-J, Kang H-J, Jung H-J, Song Y-S, Lim C-J & Park E-H, *Biomol Ther*, 16 (2008) 132.
10 Kim J H, Lee H-O, Cho Y-J, Kim J, Chun J, Choi J, Lee Y & Jung W H, *PLoS ONE*, 9 (2014) e89122.
11 Ngarmsak M, Delaquis P, Toivonen P, Ngarmsak T, Ooraikul B & Mazza G, *J Food Prot*, 69 (2006) 1724.
12 Taboonpong S, Kiratipaiboon C, Phiboonchaiyanan P P, Junthongjin P, Trithossadech P & Chanvorachote P, *Thai J Pharm Sci*, 41 (2017) 47.
13 Xu C, Zhan W, Tang X, Mo F, Fu L & Lin B, *Poly Test*, 66 (2018) 155.
14 Scipioni M, Kay G, Megson I L, Kong P & Lin T, *Eur J Med Chem*, 143 (2018) 745.
15 Yadav R, Dharamvir S & Divya Y, *Turk J Pharm Sci*, 15 (2018) 57.
16 Scipioni M, Kay G, Megson I L, Kong P & Lin T, *Med Chem Comm*, 10 (2019) 764.
17 Zhang J, Zhao L, Zhu C, Wu Z, Zhang G, Gan X, Liu D, Pan J, Hu D & Song B, *J Agric Food Chem*, 65 (2017) 4582.
18 Wu Q, Cai H, Yuan T, Li S, Gan X & Song B, *Bioorg Med Chem Lett*, 30 (2020) 127113.
19 Chadha N, Bahia M S, Kaur M & Silakari O, *Bioorg Med Chem*, 23 (2015) 2953.
20 Rocha J L F D, Rêgo M J B D M, Cavalcanti M B, Pereira M C, Rocha Pitta M G D, Oliveira P S S D, Gonçalves S M C, Duarte A L B P, Lima M D C A D, Pitta I D R, Rocha Pitta M G D, *Bio Med Res Int*, 2013 (2013) Article ID 926060.
21 Youssef A M, Sydney White M, Villanueva E B, El-Ashmawy I M & Klegeris A, *Bioorg Med Chem*, 18 (2010) 2019.
22 Albrecht U, Gördes D, Schmidt E, Thurow K, Lalk M & Langer P, *Bioorg Med Chem*, 13 (2005) 4402.
23 Jain V S, Vora D K & Ramaa C S, *Bioorg Med Chem*, 21 (2013) 1599.
24 Kim S H, Ha Y M, Moon K M, Choi Y J, Park Y J & Jeong H O, Chung K W, Lee H J, Chun P, Moon H R & Chung H Y,. *Arch Pharm Res*, 36 (2013) 1189.
25 Chinthala Y, Domatti A K, Sarfaraz A, Singh S P, Niranjana K A, Gupta N, Srinivas S K V N, Kotesh K J, Khan F, Tiwari A K & Paramjit G, *Eur J Med Chem*, 70 (2013) 308.
26 Yakaiah C, Sneha T, Shalini T, Chinde S, Kumar A D, Kumar N A, Srinivas Satya K V N, Sarfaraz A, Kumar K J, Khan F, Ashok T & Grover P, *Eur J Med Chem*, 93 (2015) 564.
27 Mallikarjun E, Suneesha D, Kumar A N, Singh A, Dutta H, Kumar J K, Srinivas S K V N, Meena A, Venkatesh B, Jain N, Sravanthi & T Radhika. *Indian J Chem*, 62 (2023) 1162.
28 Soltis M J, Yeh H J, Cole K A, Whittaker N, Wersto R P & Kohn E C, *Drug Meta Disp*, 24 (1996) 799.
29 Shareghi-Boroujeni D. IRaji A, Mojtabavi S, Faramarzi M A, Akbarzadeh T & Saeedi M, *Bioorg Chem*, 111 (2021) 104869.
30 Devendar P, Niranjana K A, Srinivas S K V N, Kumar K J, Singh S, Meena A, Misra P & Luqman S, *J Heterocycl Chem*, 58 (2021) 2090.
31 Komuraiah B, Kumar N A, Srinivas S K V N, Kumar K J, Chinde S, Kumar A D, Kumar Y, Grover P, Ashok T & Khan F, *J Heterocycl Chem*, 58 (2021) 2078.
32 Yakaiah C, Manjulatha K, Sharma P, Srinivas S K V N, Jonnala K, Kumar N A, Khan F & Setty O H, *J Heterocycl Chem*, 53 (2016) 1902.
33 Devendar P, Kumar A N, Srinivas S K V N & Kumar J K, *Indian J Chem*. 61 (2022) 51.
34 Gazolla P A R, Aguiar D A R, Costa M C A, Oliveira O V, Costa A V, Da Silva C M, Do Nascimento C J, Junker J, Ferreira R S, De Oliveira F M, Vaz B G, Do Carmo P H F, Santos D A, Ferreira M M C & Teixeira R R, *Arch Pharm (Weinheim)*, 356 (2023) e2200653.
35 Kolb H C & Sharpless K B, *Drug Disc Today*, 8 (2003) 1128.
36 Zhao T, Mu X & You Q, *Oncotarget*, 8 (2017) 53819.
37 Qian S, Wei Z, Yang W, Huang J, Yang Y & Wang J, *Front Oncol*, 12 (2022) 985363.
38 Williams M M & Cook R S, *Oncotarget*, 6 (2015) 3519.
39 Trask D K, Wolf G T, Bradford C R, Fisher S G, Devaney K, Johnson M, Singleton T & Wicha M, *The Laryngoscope*, 112 (2002) 638.
40 Singh A, Mishra A, Meena A, Mishra N & Luqman S, *J Biomol Struc Dyn*, 42 (2023) 7917.
41 Mathur A, Singh A, Hussain Y, Mishra A, Meena A, Mishra N & Luqman S, *Int J Biolog Macromol*, 257 (2024) 127945.
42 Ghose A K, Viswanadhan V N & Wendoloski J J, *J Comb Chem*, 1 (1999) 55.
43 Veber D F, Johnson S R, Cheng H-Y, Smith B R, Ward K W & Kopple K D, *J Med Chem*, 45 (2002) 2615.
44 Egan W J, Merz K M & Baldwin J J,. Prediction of Drug Absorption Using Multivariate Statistics. *Journal of Medicinal Chemistry*, 43 (2000) 3867.
45 Muegge I, Heald S L & Brittelli D, *J Med Chem*, 44 (2001) 1841.
46 Pires D E V, Blundell T L & Ascher D B, *J Med Chem*, 58 (2015) 4066.